Journal of Nanoscience and Nanotechnology
Vol. 14, 3584–3587, 2014
www.aspbs.com/jnn

Ultraviolet-Enhanced Upconversion Emission Mechanism of Tm^{3+} in YF_3:Yb^{3+}, Tm^{3+} Nanocrystals

Jisen Zhang*, Liguo Zhang, Jianyue Ren, Liping Zhang, and Shaozhe Lu

Changchun Institute of Optics, Fine Mechanics and Physics, Chinese Academy of Sciences, 3888 Dongnanhu Street Changchun, 130033, P. R. China

Dependences of the spectral profiles on the both Tm^{3+}- and Yb^{3+} additive amounts were presented. Further, the temporal evolution of Tm^{3+} luminescence in the nanocrystals was explored. Enhanced ultraviolet emissions with Tm^{3+} upconversion were investigated in the $Y_{0.800-x}F_3$:$Yb^{3+}_{0.200}$, Tm^{3+}_x, nanocrystal samples following excitation with 980 nm. The emissions can be attributed to the transitions of $^1G_4 \rightarrow {}^3H_6$, $^1D_2 \rightarrow {}^3F_4$ or $^3H_6$ and ($^3P_0$ and $^1I_6$) $\rightarrow {}^3F_4$ or $^3H_6$. A detailed energy-transition scheme was proposed and described well the ultraviolet-enhanced upconversion of Tm^{3+} and the energy-transfer processes from Yb^{3+} to Tm^{3+} based on energy-matching conditions.

Keywords: Rare-Earth, Nanocrystal, Energy Transfer, Upconversion.

1. INTRODUCTION

Investigations on optical microresonators with dimensions between 0.1∼10 μm, liquid droplets, polymer spheres, and F-P microcavities with dielectric mirrors as examples of microresonators, have attracted much attention in a wide variety of condensed matter systems.[1] Interactions between atoms and leaky optical cavities have led to observations of enhanced or inhibited spontaneous emission[2] with which one can make some phenomena accessible for study in condensed matter systems (seeing Ref. [1]). Dimensions of nanoparticles are able to be in the order of the wavelength of various wave phenomena. Therefore, at least theoretically, nanoparticles can be viewed as a boundary value problem, and it becomes obvious that, as resonators, those strongly affect their physical properties.[3] So nanoparticles with dimensions in the range of 0.1∼10 μm could be regarded as an optical microcavity.[4]

Due to the need for optical data storage, color displays, infrared (IR) sensors, environmental monitoring, and developing miniaturized and UV-lasing solid-state devices with upconversion processes, etc., rare-earth (RE)-doped upconversion (UC) materials have been widely explored since 1960s.[5∼9] Fluorides have wide applications in optics as windows, lenses, scintillation crystals,[10] and also as hosts for RE ions exhibiting excellent frequency UC features (seeing Ref. [5]). For past two decades, various RE-doped fluoride nanomaterials have been purposefully prepared because of interesting optical properties, especially a series of luminescent nanomaterials based on near IR to ultraviolet (UV) upconversion (UC) processes of Tm^{3+} have been presented. Moreover, considerable efforts have been devoted to further improving the UC emission performances of these materials in recent years.[11∼13] In more recent years, Upconversion nanoparticles have been hot for Biological application and solar cell enhancement.[14–16]

In this article, $Y_{0.800-x}F_3$:$Yb^{3+}_{0.200}$, Tm^{3+}_x nanoparticles were prepared and the strongly enhanced emissions at near-UV wavelength were observed. The results showed that the near-UV enhancement sensitively depended on the amount of both Tm^{3+} and Yb^{3+} additives. The experimental results revealed that it would be promising to apply the fluoride nanomaterials doped by rare-earth ions into searching for short-wavelength solid-state lasing materials. However, for the nanocrystals, there have been not any satisfying explains for the upconversion process mechanisms with enhanced UV UC emissions of Tm^{3+}, so it is very necessary and valuable to explore the mechanisms.

2. EXPERIMENTAL DETAILS

2.1. Synthesis and Sample Preparation

The synthesis of $Y_{0.800-x}F_3$:$Yb^{3+}_{0.200}$, Tm^{3+}_x (x = 0.001, 0.002, 0.003, 0.005) nanocrystals was elaborated on a typical preparation procedure based on the $Y_{0.795}F_3$:$Yb^{3+}_{0.200}$,

*Author to whom correspondence should be addressed.

1533-4880/2014/14/3584/004 doi:10.1166/jnn.2014.7951

$Tm^{3+}_{0.005}$ nanocrystal. Firstly, the original materials were all analytical reagents, and 5.95 mmol Y_2O_3 (99.99%), 2 mmol Yb_2O_3 (99.99%) and 0.05 mmol Tm_2O_3 (99.99%) were dissolved in hydrochloric acid (HCl, 37%) together at 60–70 °C to form clear solutions (CS), then hydrofluoric acid (HF, 40%) was added dropwise into CS to obtain turbid solution while stirring with a magnetic force stirrer. After being continuously stirred for more than 0.5 h, the colloidal solution was achieved and transferred into two 50 mL Teflonlined autoclaves in stainless steel kettle and treated at 130 °C for 12 h. After cooling to room temperature naturally, the upper clear solution was discarded and the remainder was isolated by centrifugation. The centrifugal remainder was washed with deionized water by centrifugation for at least 3 times. After dried in vacuum at 60 °C for 6 h, the resulting white powder was obtained. However, the white powder had hardly UC emissions under 980-nm excitation. After annealing for 1 h under an Ar atmosphere at 600 °C, the sample emitting bright blue and intense UV light under 980-nm excitation was obtained.

The bulk samples were prepared from analytical reagents: Y_2O_3 (99.99%), Tm_2O_3 (99.99%), and Yb_2O_3 (99.99%). 20%Yb^{3+}, 0.3%Tm^{3+} co-doped $NaYF_4$ was synthesized through a co-precipitation method and a calcining procedure. Stoichiometric Y_2O_3, Tm_2O_3 and Yb_2O_3 were dissolved in hydrochloric acid (37%) at elevated temperature with an electric cooker (800 W) to form clear solution. Then hydrofluoric acid (40%) was added dropwise into the clear solution to form colloidal solution while stirring with a magnetic stirrer. The upper clear solution was discarded and the remainder was dried at 110 °C for 3 h. After calcined at 800 °C for 2 h in an argon atmosphere, the bulk sample was obtained.

2.2. Spectral Measurements

To observe the crystallization phase, XRD analysis was carried out with Rigaku RU-200b powder diffractometer using Ni-filtered CuK_α radiation with $\lambda = 0.15406$ nm. The size and the morphology were characterized by Hitachi S-4800 field-emission scanning-electron microscopy (FE-SEM). UC emission spectra were recorded with Hitachi F-4500 fluorescence spectrophotometer. The lifetime of Tm^{3+}:$^1D_2$ state was measured with Sunlite OPO from Continuum (Repeat frequency, 10 Hz; Pulse width, 6 ns), and Triax550 spectrometer from JY and TDS3052 oscillograph from Tektronix, respectively. All measurements were performed at room temperature.

3. RESULTS AND DISCUSSION

Firstly, the XRD pattern of the annealed $Y_{0.795}F_3$:$Yb^{3+}_{0.020}$, $Tm^{3+}_{0.005}$ sample was taken. Figure 1 shows an orthorhombic YF_3 phase with the space group Pnma (62) comparing with the standard data of YF_3 crystal (JCPDS 74-0911). FE-SEM exhibits the morphology of the samples. It is

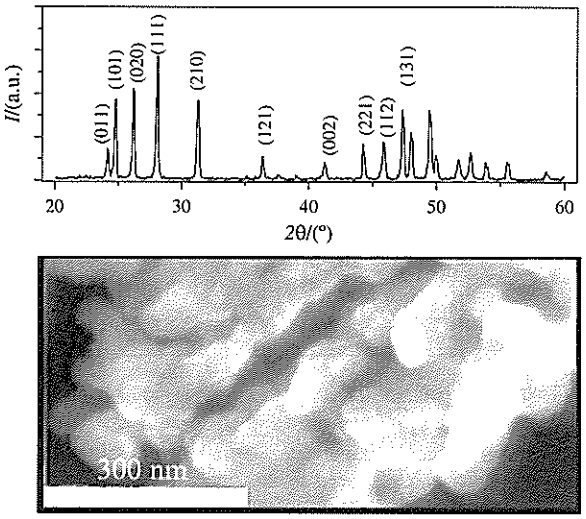

Figure 1. XRD pattern and FE-SEM image of the annealed $Y_{0.795}F_3$:$Yb^{3+}_{0.020}$, $Tm^{3+}_{0.005}$ nanocrystal.

obvious that the samples are composed of aggregated particles with an average size of about 150 nm.

It can be noted that, though the blue luminescence are always observed by naked eyes, these spectrum profiles would like to concentrate the UC light emissions on the UV regions with increasing the amount of doped Tm^{3+} in all nanocrystal samples with $Y_{0.795-x}F_3$:$Yb^{3+}_{0.020}$, Tm^{3+}_x following the excitation with 980-nm laser diode (LD) as shown in Figure 2. Comparing the nanocrystals with the bulk sample at the same Tm^{3+} doping amount in Figure 3, for the enhanced $^1I_6 \rightarrow {}^3F_4$, $^1D_2 \rightarrow {}^3H_6$ and $^1D_2 \rightarrow {}^3F_4$ radiation transition the dominant UC transition mechanism do not originate from the interactions caused by increasing the Tm^{3+}-doping amount between Tm^{3+} and Tm^{3+}, which make $^1D_2$ be efficiently populated with the $(^1G_4, {}^3H_4) \rightarrow (^1D_2, {}^3F_4)$[25] or $(^3H_6, {}^1G_4) \rightarrow (^1D_2, {}^3F_4)$[14] cross-relaxation process as shown in the inset in right-hand side of Figure 3. So, there is no doubt that the nanodimension[13, 17~23] plays a key role for the UC processes of populating $^1D_2$ and $^1I_6$ state in effect. It is well known that nanoparticles with sizes in the range of 100~1000 nm are regarded as an optical microcavity. For the microcavities under discussion here, the frequency-dependent mode density of such a cavity is characterized by a series of wide delta function at the cavity resonances because there is inevitably some leakage of radiation due to output coupling. As Tm^{3+} transition frequency does not overlap a cavity mode, the transition, such as $^1G_4 \rightarrow {}^3H_6$ radiation in Figure 4, will be inhibited. On the other hand, if Tm^{3+} transitions, such as both $^1I_6 \rightarrow {}^3F_4$ and $^1D_2 \rightarrow {}^3H_6$ radiation transitions in Figure 4, are on resonance with the cavity, then it can radiate a photon faster than it could in free space. Furthermore, as shown in Figure 4, $^1G_4 \rightarrow {}^3H_6$ radiation transition intensity basically keeps unchanged, while the $^1I_6 \rightarrow {}^3H_6$, $^1I_6 \rightarrow {}^3F_4$, $^1D_2 \rightarrow {}^3H_6$, and $^1D_2 \rightarrow {}^3F_4$ transition gradually become dominant with increasing the

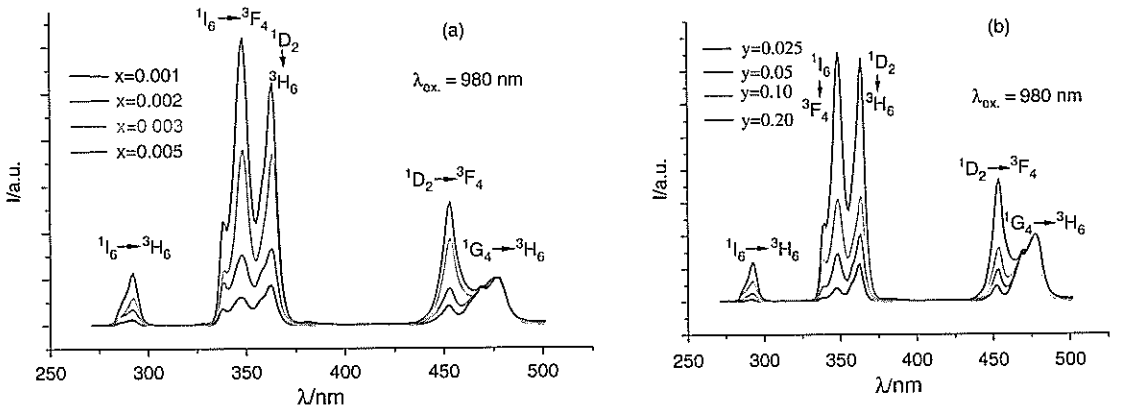

Figure 2. (a) Upconversed emission spectra of Tm^{3+} in $Y_{0.800-y}F_3$:$Yb^{3+}_{0.020}$, Tm^{3+}_x nanocrystals annealed at 600 °Cl; (b) Dependence of Tm^{3+} upconversion emissions on Yb^{3+}-doped amount the in $Y_{1-0.003-x}Yb_xTm_{0.003}F_3$ nanocrystals.

Tm^{3+}-doped amount, respectively. It is conceivable that, in the nanocrystal microcavities, only the radiation transition frequencies of $^1I_6 \rightarrow {}^3F_4$, $^1D_2 \rightarrow {}^3H_6$, and $^1D_2 \rightarrow {}^3F_4$ could well match up to the cavity mode established with the 150 nm particles, and that of $^1G_4 \rightarrow {}^3H_6$ could not do, leading to the $^1I_6 \rightarrow {}^3F_4$, $^1D_2 \rightarrow {}^3H_6$, and $^1D_2 \rightarrow {}^3F_4$ radiation transition being enhanced and the $^1G_4 \rightarrow {}^3H_6$'s inhibited. In fact, in contrast to the bulk sample, as shown in Table I, the radiation transition lifetime of Tm^{3+} $^1I_6$ and $^1D_2$ state clearly decreased.

To further explore the mechanism of the UC emissions in the nanocrystal samples, the temporal evolution of Tm^{3+} luminescence in nanocrystal and bulk samples is investigated and the lifetimes for the representative emissions (362 nm and 347 nm) from $^1D_2$ and $^1I_6$ are measured, and the decay curves can be fitted well into an exponential function as $I = A_0 \exp(-t/\tau)$. In contrast to the bulk sample, as shown in Table I, the radiation transition lifetime of Tm^{3+1} I_6 and $^1D_2$ state clearly decreased. In a word, it is suggested that, by the influences of the cavity effect on the lifetimes of Tm^{3+} excited states, the enhanced UC UV emissions of Tm^{3+} would be induced.

To visually describe the energy-transfer processes from Yb^{3+} to Tm^{3+} to Tm^{3+} well, an energy-level schemes of Yb^{3+} and Tm^{3+} and the processes of UC excitation and emissions are set up, as shown in Figure 5. It is apparent that, following the excitation with 980 nm, the five-photon processes is necessary to populate the $^1I_6$ state of Tm^{3+}, that is, the efficient UC emissions of Tm^{3+} strongly depend on the population of $^1I_6$ state. It is sure that the lifetime $^1G_4$ and $^1D_2$ state plays a uniquely important role in the

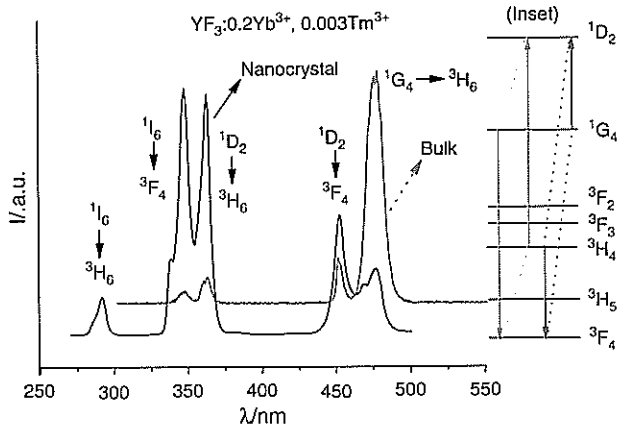

Figure 3. Upconversion emission spectrum of $Y_{0.798}F_3$:$Yb^{3+}_{0.020}$, $Tm^{3+}_{0.002}$ nanocrystal annealed at 600 °C and $Y_{0.798}F_3$:$Yb^{3+}_{0.020}$, $Tm^{3+}_{0.002}$ bulk material, respectively. Inset means schematic representation of the cross-relaxation processes populating the $^1D_2$ state with Tm^{3+} $[(^1G_4, {}^3H_4) \rightarrow (^1D_2, {}^3F_4)]$ and $[(^3H_6, {}^1G_4) \rightarrow (^1D_2, {}^3F_4)]$ in higher Tm^{3+}-doped nanocrystals.

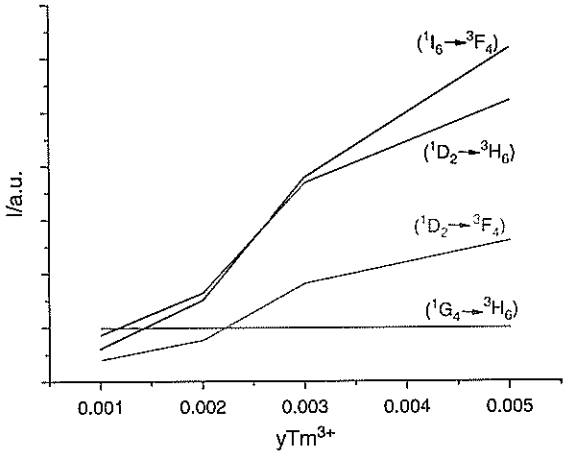

Figure 4. Dependence of upconversed emission intensity on Tm^{3+}-doped amount in $Y_{0.800-y}F_3$:$Yb^{3+}_{0.020}$, Tm^{3+}_x (x = 0.001, 0.002, 0.003, 0.005) nanocrystals, respectively.

Table I. Luminescence lifetimes of Tm^{3+} states in $Y_{0.795}F_3$:$Yb^{3+}_{0.2}$, $Tm^{3+}_{0.005}$

Peak value nm	347($^1I_6 \rightarrow {}^3F_4$)	362($^1D_2 \rightarrow {}^3F_6$)
τ/μs		
Nanocrystal	141	184
Bulk	870	670

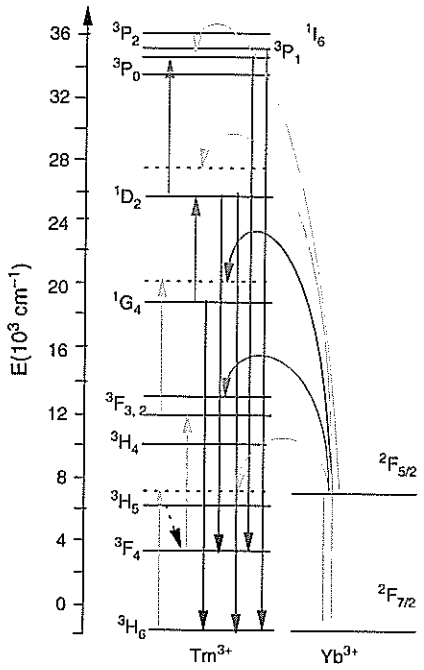

Figure 5. Level diagrams of Yb^{3+} and Tm^{3+} in $Y_{0.800-x}F_3$:$Yb^{3+}_{0.020}$, Tm^{3+}_x nanocrystals annealed at 600 °C and schematic upconversion processes following 980 nm LD excitation.

efficient energy transfer processes. In fact, the nanocrystal diameter is less than the half wavelengths of the $^1G_4 \rightarrow {}^3H_6$ radiation transitions, which makes the $^1G_4$ state transition rates decrease rapidly (seeing Ref. [17]), leading to more efficient population at $^1D_2$ state. The obtained emission spectra are direct proof of the validity for the explanation. The scale of nanocrystals has worthful effects on the enhanced UV upconversion emissions of Tm^{3+}.

4. CONCLUSIONS

The investigation ideas are to explore the mechanism of the enhancement of *n*-photon UC transitions with the nanodimension materials and UV-emitting materials following the excitation with near-infrared LD. The experiments show that the $Y_{0.745}F_3$:$Yb^{3+}_{0.200}$, $Tm^{3+}_{0.005}$ nanocrystal sample is able to be synthesized by a hydrothermal method, and intense UV UC emissions are observed following 980 nm LD excitation. Based on the microcavity effect, it is hoped that the nanocrystal materials could be possibly applied to manufacture miniaturized and ultraviolet (UV)-lasing solid-state devices with UC.

Acknowledgment: This work is supported by National Science Foundation of China under Grant Nos. 11174276, 11174278.

References and Notes

1. R. K. Chang and A. J. Campillo, Optical Processes in Microcavities, World Scientific, Singapore (**1996**).
2. S. Haroche and D. Kleppner, *Physics Today* 42, 24 (**1989**).
3. C. Cao, *J. Nanosci. Nanotechnol.* 11, 9701 (**2011**).
4. M. Giersig and G. B. Khomutov, Nanomaterials for Application in Medicine and Biology, Springer, Netherlands (**2008**), Vol. 179.
5. F. Auzel, *Proc. IEEE* 61, 758 (**1973**); F. Auzel, *Chem. Rev.* 104, 139 (**2004**).
6. X. Zhang, C. Serrano, E. Daran, F. Lahoz, G. Lacoste, and A. Muñoz-Yagüe, *Phys. Rev. B* 62, 4446 (**2000**).
7. C. Y. Cao, W. P. Qin, J. S. Zhang, Y. Wang, G. F. Wang, G. D. Wei, P. F. Zhu, L. L. Wang, and L. Z. Jin, *Opt. Commun.* 281, 1716 (**2008**).
8. Y. F. Bai, Y. X. Wang, G. Y. Peng, W. Zhang, Y. K. Wang, K. Yang, X. R. Zhang, and Y. L. Song, *Opt. Commun.* 282, 1922 (**2009**).
9. X. C. Yu, F. Song, W. T. Wang, L. J. Luo, C. G. Ming, Z. Z. Cheng, L. Han, T. Q. Sun, H. Yu, and J. G. Tian, *Opt. Commun.* 282, 2045 (**2009**).
10. E. Slunga, B. Cederwall, E. Ideguchi, A. Kerek, W. Klamra, J. Van der Marel, D. Novak, and L.-O. Norlin, *Nucl. Instrum. Methods Phys. Res. Sect. A* 469, 70 (**2001**).
11. C. Cao, W. Qin, J. Zhang, P. Zhu, G. Wei, G. Wang, R. Kim, and L. Wang *Opt. Lett.* 33, 857 (**2008**).
12. W. Qin, C. Cao, L. Wang, J. Zhang, D. Zhang, K. Zheng, Y. Wang, G. Wei, G. Wang, P. Zhu, and R. Kim, *Opt. Lett.* 33, 2167 (**2008**).
13. J. Zhang, L. Zhang, S. Lu, and W. Qin, *J. Nanosci. Nanotechnol.* 10, 1974 (**2010**).
14. L. Yongsheng, J. Qiang, and C. Xueyuan, *Rev. Nanosci. Nanotechnol.* 1, 163 (**2012**).
15. W. Chen, *J. Nanosci. Nanotechnol.* 8, 1019 (**2008**).
16. S.-M. Liu, W. Chen, and Z.-G. Wang, *J. Nanosci. Nanotechnol.* 10,1418 (**2010**).
17. F. Pandozzi, F. Vetrone, J.-C. Boyer, R. Naccache, J. A. Capobianco, A. Speghini, and M. Bettinelli, *J. Phys. Chem. B* 109, 17400 (**2005**).
18. F. Auzel, *Compt. Rend. Acad. Sci.* 263B, 819 (**1996**).
19. F. W. Ostermayer, J. J. P. Van der ziel, H. M. Marcos, L. C. Van Uilert, and J. E. Geusic, *Phys. Rev. B* 3, 2698 (**1971**).
20. Y. Mita, T. M. T. Ide, and H. Yamamoto, *J. Appl. Phys.* 85, 4160 (**1999**).
21. H. Chew, *Phys. Rev. A* 38, 3410 (**1988**).
22. Q. Huang, J. Yu, E. Ma, and K. Lin, *J. Phys. Chem. C* 114, 4719 (**2010**).
23. T. Riedener, H. U. Güdel, G. C. Valley, and R. A. McFarlane, *J. Lumin.* 63, 327 (**1995**).

Received: 3 August 2012. Accepted: 1 December 2012.